Article

Cell

# Multisensory Signaling Shapes Vestibulo-Motor Circuit Specificity

## Graphical Abstract

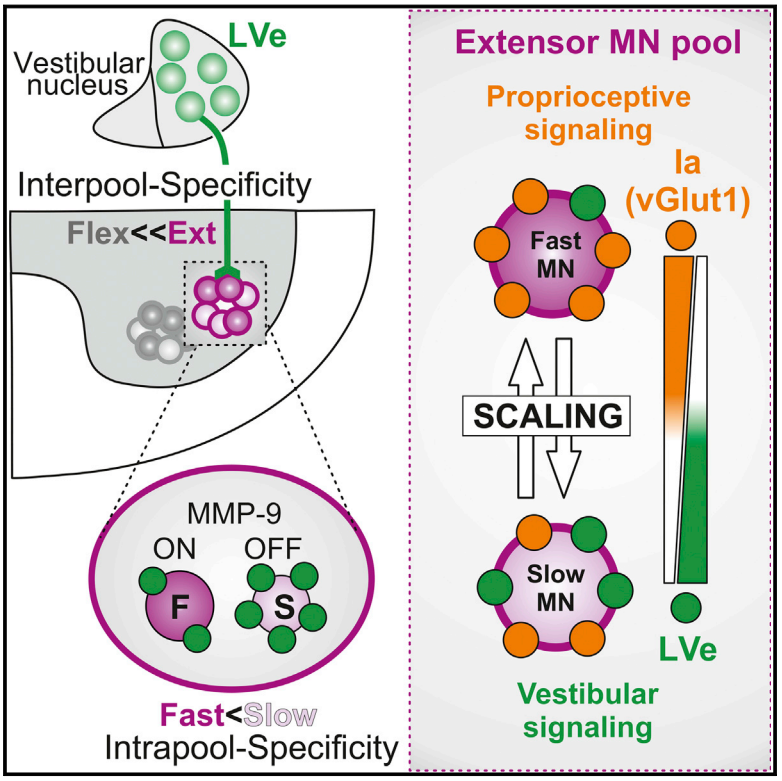


## Highlights

- Preferential targeting of vestibular input to slow motor neurons of extensor pools
- Vestibular input specificity to motor neurons assembled by developmental refinement
- Vestibular and proprioceptive input to motor neuron subtypes inversely correlated
- Proprioceptive circuits shape vestibular input to specific motor neuron subtypes

## Authors

Emanuela Basaldella, Aya Takeoka, Markus Sigrist, Silvia Arber

## Correspondence

silvia.arber@unibas.ch

## In Brief

Vestibular and proprioceptive system signaling controls body balance by targeting motor neurons regulating functionally distinct muscles and fiber types. Their synaptic inputs at the final step of motor output processing are shaped by functional interactions between these two sensory systems.

Basaldella et al., 2015, Cell *163*, 301–312
October 8, 2015 
http://dx.doi.org/10.1016/j.cell.2015.09.023

CellPress

Article

Cell

# Multisensory Signaling Shapes Vestibulo-Motor Circuit Specificity

Emanuela Basaldella,[1,2] Aya Takeoka,[1,2] Markus Sigrist,[1,2] and Silvia Arber[1,2,*]
[1]Biozentrum, Department of Cell Biology, University of Basel, 4056 Basel, Switzerland
[2]Friedrich Miescher Institute for Biomedical Research, 4058 Basel, Switzerland
*Correspondence: silvia.arber@unibas.ch
http://dx.doi.org/10.1016/j.cell.2015.09.023

## SUMMARY

The ability to continuously adjust posture and balance is necessary for reliable motor behavior. Vestibular and proprioceptive systems influence postural adjustments during movement by signaling functionally complementary sensory information. Using viral tracing and mouse genetics, we reveal two patterns of synaptic specificity between brainstem vestibular neurons and spinal motor neurons, established through distinct mechanisms. First, vestibular input targets preferentially extensor over flexor motor pools, a pattern established by developmental refinement in part controlled by vestibular signaling. Second, vestibular input targets slow-twitch over fast motor neuron subtypes within extensor pools, while proprioceptors exhibit inversely correlated connectivity profiles. Genetic manipulations affecting the functionality of proprioceptive feedback circuits lead to adjustments in vestibular input to motor neuron subtypes counterbalancing the imposed changes, without changing the sparse vestibular input to flexor pools. Thus, two sensory signaling systems interact to establish complementary synaptic input patterns to the final site of motor output processing.

## INTRODUCTION

Descending motor control pathways are essential to regulate spinal circuits involved in movement (Grillner and Dubuc, 1988; Lundberg, 1975). Specificity of synaptic connections between upper motor control centers and the spinal output system provides the anatomical substrate to implement movement variety and precision. As animals grow up, they engage in progressively more diverse and refined motor behaviors, paralleling the establishment of functionally mature descending input to spinal circuits. Despite the importance of this descending connection matrix, the organization of its key components and especially the elucidation of developmental mechanisms involved in its establishment are still under intense investigation.

The ability to continuously adjust posture and balance during movement matures at postnatal stages in mammals (Brown, 1981; Geisler et al., 1993). Due to the importance of these adaptive mechanisms for the execution of highly diverse motor programs, circuits steering body stabilization must exhibit a high degree of tuning flexibility. Two parallel and functionally complementary sensory signaling systems play key roles in this process. In the vestibular system, one central sensory organ in the inner ear monitors linear and rotational acceleration and provides input to the vestibular nucleus of the brainstem (Angelaki and Cullen, 2008; Brodal and Pompeiano, 1957). Descending vestibulo-spinal projection neurons transmit this information to spinal circuits to provide postural stability (Grillner et al., 1970; Lund and Pompeiano, 1968; Shinoda et al., 1988; Wilson and Yoshida, 1968). The somatosensory system represents a complementary signaling system in which sense organs are distributed throughout the entire body (Abraira and Ginty, 2013; Brown, 1981; Matthews, 1981). Within this system, proprioceptive sensory neurons located in dorsal root ganglia (DRG) monitor self-generated actions and extrinsic perturbations in the periphery. Of these, muscle spindle afferents report the state of muscle contraction from specific sites in the periphery directly to spinal motor neurons through monosynaptic reflex arcs (Brown, 1981; Eccles et al., 1957; Windhorst, 2007).

Revealing the organization of synaptic connections to spinal motor neurons is crucial to understand how vestibular and proprioceptive information influences motor output. Studies in the adult cat provide the first evidence that vestibular neurons preferentially target extensor motor neuron pools (Grillner et al., 1970). In contrast, proprioceptors contact motor neurons of most pools in the spinal cord. A motor pool receives direct synaptic input from muscle spindle afferents supplying the same or synergistic muscles, but not from afferents innervating antagonistic muscles (Eccles et al., 1957; Mears and Frank, 1997). Thus, both extensor and flexor motor neuron pools get direct proprioceptive input but in highly specific configurations, whereas direct vestibular input seems to be preferentially targeted to extensor motor neurons in line with its body-stabilizing and anti-gravitational function. Beyond their connectivity profiles, vestibular and proprioceptive systems also interact functionally with each other and can contribute to both enhancement or depression of responses in motor neurons (Grillner et al., 1970).

Less is known about the mechanisms guiding developmental assembly of these two sensory systems. Specific connectivity between proprioceptors and motor neurons in the same reflex arc is already present at early postnatal developmental stages in mice (Mears and Frank, 1997) and activity-independent in

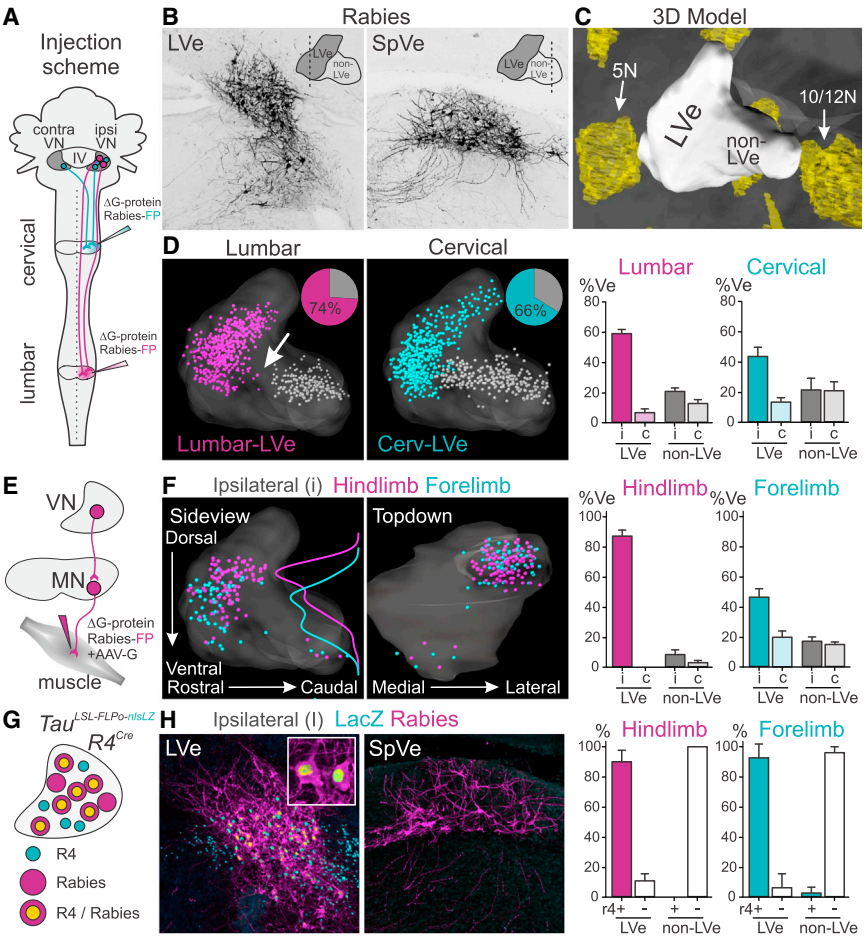


**Figure 1. Spatial Distribution of Vestibular Neurons Regulating Spinal Motor Neurons**

(A) Unilateral injections of G-protein-deleted Rabies viruses encoding fluorescent proteins (FP) into cervical and lumbar spinal cord to assess the position of vestibular neurons in the brainstem.

(B) Representative coronal sections at the level of the lateral vestibular nucleus (LVe; left) and spinal vestibular nucleus (SpVe; right) ipsilateral to injection.

(C) Three-dimensional model of the vestibular nucleus used for digital reconstructions, surrounded by cranial motor nuclei 5N and 10/12N.

(D) Ipsilateral side view of digital 3D vestibular nucleus reconstructions derived from lumbar (left) and cervical (middle) spinal injections (colored neurons reside in, gray neurons outside LVe). Pie charts in upper right corners show percentages of LVe neurons. Right: quantification of lumbar and cervical projection neuron composition in Ve nucleus, stratified by ipsi- and contralateral as well as LVe and non-LVe residence.

(E) Strategy for monosynaptic rabies tracing experiments to determine connectivity between vestibular and motor neurons.

(F) Side- (left) and top-down (middle) view of vestibular nucleus ipsilateral to muscle injection, depicting the position of vestibular neurons connected to FL- (cyan) and HL- (purple) innervating motor neurons. Density curves for HL and FL premotor neuron distributions along the dorsoventral axis superimposed to the ipsilateral side-view panel. Right: quantification of positional distribution as in (D).

(G) Genetic strategy to mark LVe neurons by developmental origin. *R4::Cre* mice are crossed to *Tau*-reporter mice for conditional expression of nls-LacZ and FLPo expression to assess the percentage of premotor vestibular neurons marked by R4-origin.

(H) Most HL- or FL-premotor (Rabies$^{ON}$) neurons in LVe are marked by *R4::Cre*-induced LacZ, whereas premotor neurons residing in SpVe do not carry this tag (left, middle: exemplary images; right: quantification).

frogs (Frank, 1990). In the vestibular system, transient developmental perturbations affect motor behavior in several species (Geisler and Gramsbergen, 1998; Moorman et al., 2002; Van Cleave and Shall, 2006; Walton et al., 2005), raising the possibility that the assembly of the vestibular system might be plastic. Together, these observations provide first hints that even though proprioceptive and vestibular systems both functionally converge on motor neurons, their organization and developmental assembly mechanisms might be distinct. Moreover, whether and how they influence each other to establish mature functionality is unknown.

In this study, we exploit intersectional viral tracing technology and mouse genetics to reveal that vestibulo-spinal projection neurons in the brainstem exhibit connection specificity to motor neurons. We demonstrate that they do not only target extensor over flexor motor neuron pools, but that within extensor pools, they preferentially connect to slow over fast motor neurons. We find that connectivity profiles arise gradually at postnatal developmental stages, paralleling postural maturation. Genetic perturbation of vestibular signaling leads to interpool connectivity defects, whereas proprioceptive feedback circuit alterations induce specific connectivity shifts in synaptic scaling of vestibular input to motor neuron subtypes. These findings support a model in which two major sensory signaling systems interact at the final motor output step to establish specific connectivity profiles by complementary cross-modal signaling.

## RESULTS

### Spatial Organization of Spinal Projection Neurons in the Vestibular Nucleus

To delineate the position of vestibular neurons with spinal projections, we performed unilateral intraspinal injections of G-protein-deficient rabies viruses encoding fluorescent marker proteins (FP) (Rab-FP) (Wickersham et al., 2007) (Figures 1A and 1B). We found that in a three-dimensional digital brainstem model (Figure 1C), vestibular neurons with lumbar projections were preferentially located ipsilaterally, with dominant residence within the lateral vestibular (LVe) nucleus and with a clear spatial segregation to a caudal cluster of non-LVe neurons that were

bilaterally distributed (Figure 1D; including spinal vestibular neurons [SpVe]). Vestibular neurons projecting to cervical spinal levels also showed clear, albeit less pronounced ipsilateral residence within LVe, but occupied the vestibular nucleus continuously into caudal non-LVe territory (Figure 1D). In summary, for both lumbar and cervical vestibular projection neurons, LVe neurons exhibited a strong ipsilateral bias (Figure 1D). These findings confirm and extend findings that subgroups of mouse vestibular neurons exhibit differential projection trajectories to interact with local circuits in the spinal cord (Liang et al., 2014, 2015).

To determine the identity of vestibular neurons exerting the most direct influence on spinal motor neurons, we next assessed abundance and position of vestibular neurons with direct synaptic connections to motor neurons. We used a transsynaptic rabies virus-based approach with monosynaptic restriction (Wickersham et al., 2007) (Figure 1E). The majority of neurons with direct connections to lumbar motor neurons resided in the ipsilateral LVe nucleus, with the highest density peak more dorsal to neurons with connections to cervical motor neurons (Figure 1F).

To gain genetic access to neurons in the LVe nucleus, we applied a lineage tracing approach for neurons developmentally derived from different rhombomeric (R) origin (Figure 1G). To permanently mark R4-derived neurons, we used intersectional breeding of *R4::Cre* mice (Di Bonito et al., 2013) and the conditional neuronal reporter strain $Tau^{lox\text{-}STOP\text{-}lox\text{-}Flp\text{-}INLA}$ (Pivetta et al., 2014). This strategy labeled the majority of lumbar-projecting LVe neurons, but the R4-marker was entirely excluded from non-LVe neurons (Figure 1H), which are derived from more caudal rhombomeres (data not shown). Together, the existence of the clearly delineated ipsilateral cluster of vestibular neurons in the LVe nucleus and the access to specific targeting approaches allowed us to next dissect projection trajectory and connection specificity of these neurons to lumbar spinal circuits with precision.

## Lateral Vestibular Synaptic Input Is Biased to Extensor Motor Neurons

To reveal the descending projection trajectory and the synaptic arborization pattern of LVe neurons to the lumbar spinal cord, we performed focal injections of adeno-associated viruses (AAV) into the LVe nucleus. We used AAVs expressing tdTomato for axonal tracing and/or a fusion protein between synaptophysin and GFP or Myc (Syn-Tag) for synaptic reconstructions (Figures S1A–S1C). We found that axons descending from the LVe nucleus to the lumbar spinal cord were confined to ipsilateral white matter tracts (Figure S1D), consistent with previous experiments (Liang et al., 2014). Analysis of Syn-Tag distribution in the lumbar spinal cord revealed the highest density of synaptic terminals in lamina VIII ipsilateral to injection (Figures S1D and S2). Many Syn-Tag puncta were also detected throughout the ipsilateral ventral spinal cord below the central canal including lamina IX containing $ChAT^{ON}$ motor neurons (Figures S1D and S2). A similar distribution pattern was observed upon AAV-FRT-Syn-Tag LVe injection in *R4::Cre/* $Tau^{lox\text{-}STOP\text{-}lox\text{-}Flp\text{-}INLA}$ mice (Figure S2). Moreover, and similar to findings in the rat (Du Beau et al., 2012), the majority of $Syn\text{-}Tag^{ON}$ terminals accumulate the vesicular glutamate transporter vGlut2 (74.6%; Figure S1E), demonstrating that LVe spinal projection neurons provide excitatory input to the lumbar spinal cord.

We next assessed whether LVe input to the lumbar spinal cord exhibits synaptic specificity with respect to the identity of contacted motor neurons. We combined LVe AAV-Syn-Tag injections with retrograde tracing of motor neurons from identified hindlimb muscles (Figures 2A and S1A). We analyzed LVe input to motor neurons pools innervating the ankle extensor gastrocnemius (GS) and the ankle flexor tibialis anterior (TA), due to their functional antagonism as well as previous evidence for GS-biased vestibular synaptic input in the cat (Grillner et al., 1970). Vestibular input was also strongly biased toward the GS compared to the TA motor neuron pool in mice, a bias detected irrespective of cell body or dendritic analysis of reconstructed GS/TA motor neurons (Figures 2A and 2B).

## Lateral Vestibular Input Avoids GSL1 Motor Neuron Subtypes

Despite this striking difference in overall input between GS and TA motor neurons, we noted that LVe synaptic input to individual GS motor neurons was highly variable. While some GS motor neurons received low (GS-low) LVe input, others were targeted by high-density (GS-high) LVe input (Figures 2A and 2B). These findings suggest that not all GS motor neurons are equally favored targets for vestibular input and raise the question of the underlying reason for this variability.

Most skeletal muscles are composed of a mixture of different fiber types innervated by three functionally matched alpha motor neuron subpopulations. These motor neuron subtypes are differentially recruited during movement and include fast fatigable (FF), fatigue resistant (FR), and slow motor units (Burke, 1967; Kanning et al., 2010). In the mouse, the most lateral subcompartment of the lateral GS muscle (GSL1) is a very valuable exception to this rule in that it is innervated exclusively by FF motor neurons (Pun et al., 2006). This property allowed us to assess LVe input specifically to FF motor neurons within the GS motor pool (Figure 2C). We found that GSL1 FF motor neurons received only low-density LVe input and notably significantly less than the entire GS motor pool (Figures 2C and 2D). In addition, cell body volume values of motor neurons innervating the GSL1 compartment have a tendency to accumulate in the upper two-thirds of the distribution spectrum (Figure 2E). Nonetheless, and consistent with previous observations (Burke et al., 1982), such size range classifications are not sufficient to unambiguously assign motor neuron subtype identity. In summary, GSL1 FF motor neurons receive low-density LVe input, raising the possibility that this input is preferentially targeted to specific motor neuron subtypes within extensor pools.

## LVe Input Prefers Molecularly Defined Slow Motor Neurons in Extensor Pools

We next aimed to generalize our finding that LVe inputs might prefer slow motor neuron subtypes. Recent observations demonstrate that chondrolectin (Chodl) and matrix metalloprotease-9 (MMP-9) are expressed by fast motor neurons (Enjin et al., 2010; Kaplan et al., 2014; Leroy et al., 2014). In mice expressing the membrane marker protein placental alkaline

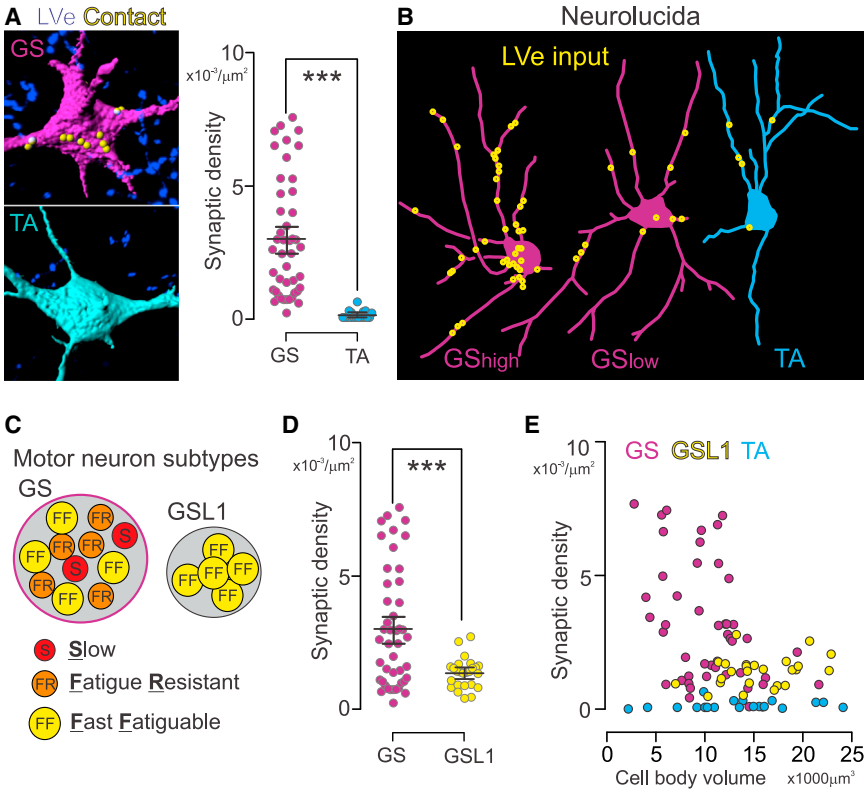


**Figure 2. Vestibular Input Stratifies by Motor Neuron Subtype and Size**

(A) Digital reconstruction and quantification of LVe synaptic input density to GS and TA motor neurons (each dot represents one motor neuron).

(B) Representative Neurolucida reconstructions of GS/TA motor neurons and LVe synaptic input (yellow). GS examples with high and low input density are shown.

(C) Motor neuron subtype composition of GS and GSL1 motor pool stratified into slow (S), FR (fatigue resistant), and FF (fast fatigable) subtypes.

(D) Quantification of synaptic density of LVe input to GS and GSL1 motor neurons (each dot represents one motor neuron).

(E) Synaptic density of LVe input to analyzed motor neurons plotted against cell body volumes.

See also Figures S1 and S2.

phosphatase (PLAP) from the *Chodl* locus (*Chodl*$^{PLAP}$) (Sakurai et al., 2013), a large majority of Chodl$^{ON}$ lumbar ChAT$^{ON}$ motor neurons in the lateral motor column (LMC) coexpressed MMP-9 (92%), and all GSL1 FF motor neurons were PLAP$^{ON}$/MMP-9$^{ON}$ (Figures 3A–3C). We first quantified LVe synaptic input density to lumbar LMC motor neurons overall in *Chodl*$^{PLAP}$ mice. Stratification of LVe input density by PLAP$^{ON}$ and PLAP$^{OFF}$ status of targeted LMC motor neurons revealed significantly lower input density to PLAP$^{ON}$ than putative alpha PLAP$^{OFF}$ motor neurons (Figures 3D and 3E). Furthermore, there was a significant inverse correlation between LVe synaptic input density and motor neuron cell body volume (Figure 3E).

To determine whether the uncovered LVe synaptic input rule based on Chodl/MMP-9 stratification also applies to motor neuron subtypes within a given extensor motor pool other than GS (Figures 2C–2E), we analyzed two more motor pools innervating extensor muscles. The ankle extensor muscle soleus (Sol) is innervated by an approximately equal number of slow and FR motor neurons in mice, but does not contain any FF motor neurons (Kaplan et al., 2014; Pun et al., 2006). Analysis of LVe input density to Sol motor neurons stratified by MMP-9 status revealed significantly lower values for MMP-9$^{ON}$ than MMP-9$^{OFF}$ Sol motor neurons (Figure 3F). Additionally, since the Sol motor pool does not contain any FF motor neurons (Pun et al., 2006), these findings indicate that slow motor neurons are not only a preferred LVe target over FF, but also over FR motor neurons. We next assessed LVe input to MMP-9 stratified motor neurons innervating the hip extensor gluteus (GL) and found that also for this pool, MMP-9$^{ON}$ populations received significantly lower input than the MMP-9$^{OFF}$ cohort (Figure 3F). Moreover, the corresponding functionally antagonistic hip flexor (Iliopsoas) motor pool showed LVe input density values similarly low as to TA flexor motor neurons (Figure 3F), thus generalizing our findings to other motor neuron pools.

Together, our experiments support a model in which synaptic input specificity of LVe neurons to lumbar LMC motor neurons is organized at different levels (Figure 3G). First, LVe axons seek out extensor over flexor motor pools as preferred synaptic targets in agreement with previous work (Grillner et al., 1970). Second, LVe synaptic contacts preferentially target slow over fast motor neuron subtypes within an extensor pool. These findings raise the question of how this synaptic specificity arises during development and what may be factors regulating its establishment.

## Developmental Refinement of Vestibular Synaptic Input Specificity to Motor Neurons

To assess synaptic input specificity of LVe neurons to lumbar motor neurons during development, we carried out spatially confined injections of AAV-Syn-Tag into the LVe nucleus early postnatally and retrogradely labeled GS or TA motor neurons (Figure 4A). The earliest time point for which it was technically possible to achieve consistent high-level Syn-Tag accumulation from LVe neurons in the lumbar spinal cord was P7. GS motor neurons at P7 receive synaptic input at densities similar to adult (Figure 4B). However, while the difference in input density between GS and TA motor neurons was already established at P7, LVe terminals frequently contacted TA motor neurons at an overall significantly higher input density than in the adult (Figure 4B). To assess during which time window the transition to mature connectivity profiles emerges, we carried out synaptic input mapping at progressively later developmental time points (Figure 4A). We found that LVe neurons still contact TA motor neurons at P11, but that developmental refinement was complete by P17 (Figure 4B).

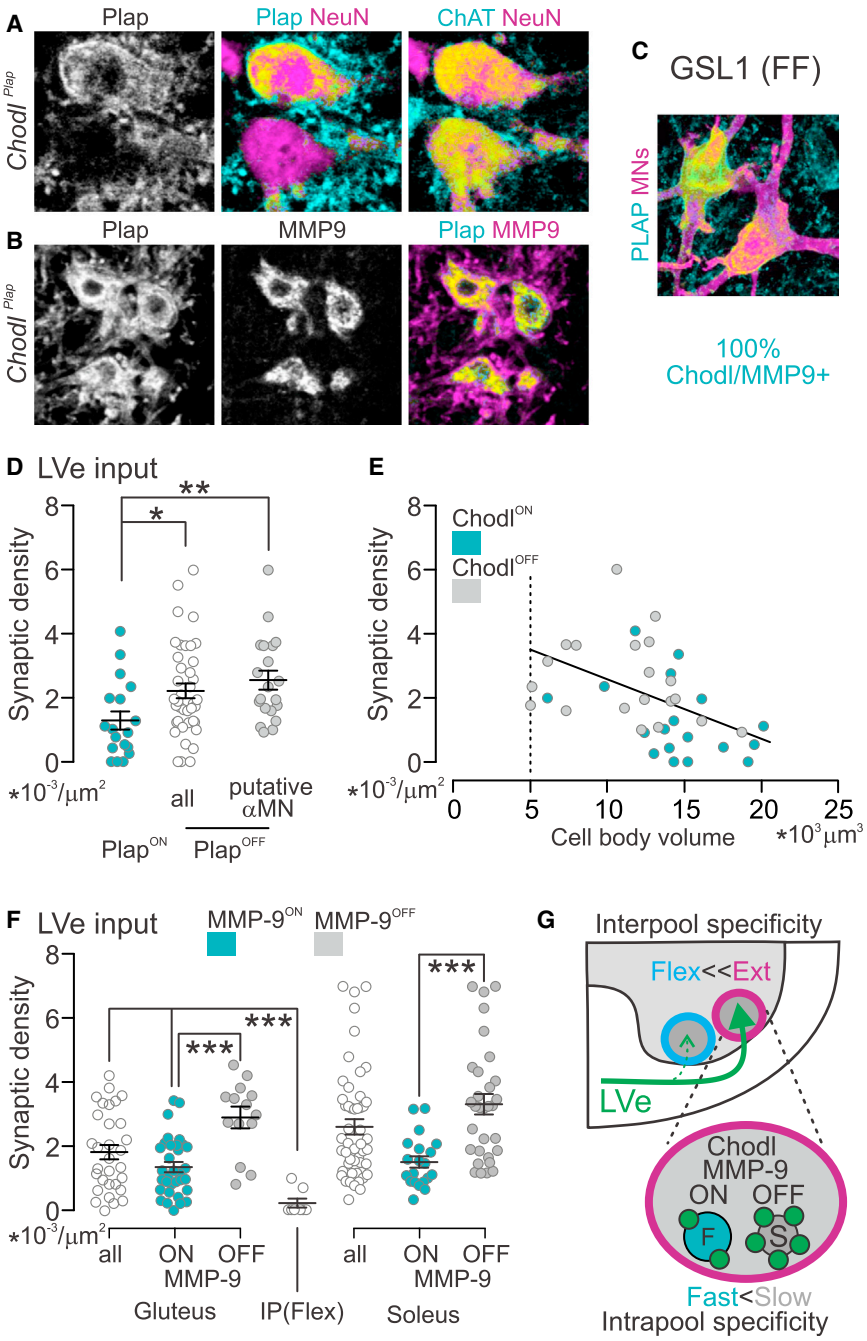


**Figure 3. Vestibular Input Preferentially Targets Putative Slow over Fast Motor Neurons**

(A and B) ChAT$^{ON}$/NeuN$^{ON}$ alpha motor neurons in the lumbar spinal cord of *ChodI$^{PLAP}$* mice fractionate into ChodI$^{ON}$ and ChodI$^{OFF}$ population, of which the ChodI$^{ON}$ neurons also express MMP-9.

(C) Retrogradely marked GSL1 FF motor neurons express ChodI.

(D) Density of LVe synaptic input to PLAP$^{ON}$, PLAP$^{OFF}$ (all, or excluding putative gamma motor neurons using a size cut-off criterion of 5,000 μm$^3$) motor neurons.

(E) Synaptic density of LVe input to PLAP$^{ON}$ and putative alpha PLAP$^{OFF}$ motor neurons analyzed in (D) plotted against cell body volumes ($r = -0.548$, $p = 0.0005$).

(F) Analysis of LVe input density for gluteus and soleus motor neurons stratified by MMP-9 expression status (cyan, MMP-9$^{ON}$; gray, MMP-9$^{OFF}$). Input to antagonistic hip flexor muscle iliopsoas (IP) is also shown.

(G) Summary diagram of synaptic specificity between LVe and motor neurons. LVe preferentially targets extensor over flexor motor pools (top, interpool specificity) and within extensor pools preferentially slow over fast motor neuron subtypes (bottom, intrapool specificity, green dots represent synapses).

To determine whether LVe contacts to TA motor neurons at early postnatal stages represent synaptic contacts, we applied monosynaptic rabies viruses to muscles innervated by GS and TA motor neurons (Figure 4C). We found that LVe neurons connect to both GS and TA motor pools at these stages, but significantly more LVe neurons were labeled after GS than TA muscle injections, at a ratio comparable to the anterograde synaptic density measurements at P11 (Figures 4D and 4E). Together, these data confirm our anterograde tracing results, demonstrating that initial developmental synaptic contacts to TA motor neurons are eliminated between P11 and P17, when they reach a mature connectivity profile (Figure 4F).

## Perturbing Vestibular Signaling Affects Establishment of Interpool Synaptic Specificity

To elucidate the mechanisms by which selectivity of vestibular input to spinal motor neurons is established, we used two different genetic models in the mouse exhibiting altered vestibular neuron signaling. We asked how these perturbations influence the establishment of mature connectivity profiles between vestibular neurons and spinal motor neurons.

We first analyzed *NADPH oxidase 3* (*Nox3*) mutant mice (Figure 5A). These mice lack mineralized particles called otoconia in the inner ear's utricle and saccule, leading to selective defects in perception of gravity and linear acceleration, but they exhibit intact semicircular canal vestibular as well as auditory sensory inputs (Paffenholz et al., 2004). Of the five known vestibular input channels, predominantly utricular or posterior semicircular canal nerve activation influences lumbar spinal circuits through the lateral vestibular tract (Uchino and Kushiro, 2011). *Nox3* mutant mice therefore exhibit congenitally altered LVe input to the lumbar spinal cord, lacking information derived from the utricular sensory input channel but not from semicircular canals.

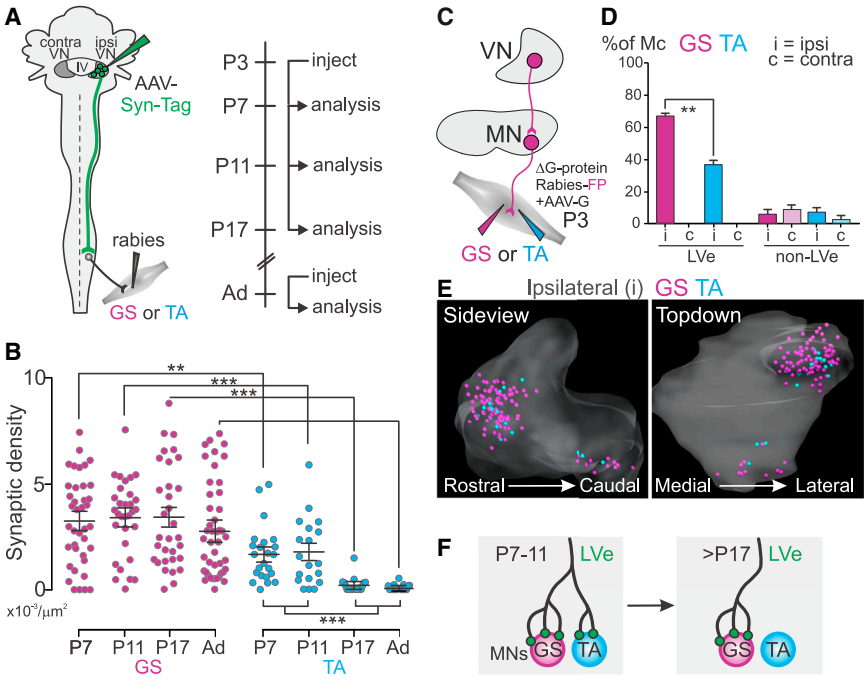


**Figure 4. Developmental Refinement of Vestibular Input to Lumbar Motor Neurons**

(A) Experimental approach used and timeline. AAV-Syn-Tag is injected into LVe of P3 (or adult) mice, followed by retrograde marking of GS or TA motor neurons by muscular tracer injections.

(B) Synaptic density of LVe input to GS and TA motor neurons at P7, P11, P17, and adult stages.

(C–E) Monosynaptic rabies tracing experiment at P3. Quantification of marked neurons in LVe and non-LVe territory (see Figure 1), both ipsi- (i) and contra- (c) lateral to muscle injection (normalized to rabies neuron number in Magnocellular nucleus). Side- and top-down view of ipsilateral vestibular reconstruction depicting GS (purple) and TA (cyan) vestibular neurons shown in (E). Neurons connected to GS or TA motor neurons were intermingled and no spatial segregation was discernable (E).

(F) Summary diagram illustrating developmental refinement process of LVe input to GS and TA motor neurons.

We first determined whether *Nox3* mutation affects the establishment of LVe synaptic inputs to the functionally antagonistic motor neuron pools GS and TA. We found that there was no difference in LVe input density to GS motor neurons between wild-type and *Nox3* mutant mice, but that TA motor neurons received LVe input at a significantly higher density in *Nox3* mutant than wild-type mice (Figure 5B). When we compared LVe synaptic input density at P11, a time point before mature connectivity profiles are reached in wild-type mice, LVe input to TA motor neurons was not different between wild-type and *Nox3* mutant mice (Figure 5B). Moreover, between P11 and adult stages in *Nox3* mutant mice, no significant refinement of LVe input to TA motor neurons occurred (Figure 5B). Together, these findings demonstrate that LVe neurons maintain aberrant synaptic input to flexor motor neurons when otholitic vestibular signaling is non-functional.

We next asked whether utricular vestibular signaling also influences LVe connectivity profiles to fast and slow motor neuron subtypes. There was no significant difference in LVe synaptic input to FF GSL1 motor neurons between wild-type and *Nox3* mutant mice (Figure 5C). We also analyzed LVe input density to Sol motor neurons stratified by MMP-9 status to distinguish between fast (MMP-9$^{ON}$) and slow (MMP-9$^{OFF}$) motor neuron subtypes. While *Nox3* mutant mice still exhibited clear intrapool differences to these motor neuron subtypes, the connectivity stratification was less pronounced than in wild-type mice (Figure 5C). Together, these findings suggest that *Nox3* mutants exhibit defects in interpool but no major intrapool LVe synaptic connectivity.

We next analyzed an intersectional mouse mutant in which the synaptic output of most LVe neurons is functionally muted from the earliest developmental stages. This genetic strategy is based on our observations that most LVe neurons projecting to lumbar spinal levels are of developmental rhombomeric origin R4 and express the glutamate transporter vGlut2. In agreement, genetic elimination of *vGlut2* from R4-derived LVe neurons (*R4$^{Cre}$::vGlut2$^{flox}$* mice) abolishes vGlut2 protein from the vast majority of spinal synapses derived from LVe neurons (Figures 5A and S3).

Since *R4$^{Cre}$::vGlut2$^{flox}$* mice have not been characterized before, we determined whether they exhibit motor behavioral deficiencies compatible with impaired LVe function. *R4$^{Cre}$::vGlut2$^{flox}$* mice executed open field navigation, grip strength, and horizontal ladder tasks similar to wild-type mice (Figure 5D). In contrast, they exhibited defects in tasks predicted to profoundly engage the vestibular system. *R4$^{Cre}$::vGlut2$^{flox}$* mice walking on a narrow beam showed significantly more slips than wild-type mice, and this phenotype was particularly pronounced on 6 mm- over 12 mm-wide beams (Figure 5D). These behavioral experiments suggest that elimination of *vGlut2* from R4-derived LVe neurons affects vestibular function and leads to motor defects attributable to such perturbations.

We next assessed synaptic input to TA motor neurons in these mice and found a significantly higher synaptic input density compared to wild-type (Figure 5B), similar to the phenotype in *Nox3* mutant mice. Lastly, also similar to our observations in *Nox3* mutant mice, we found no differences in LVe synaptic input to GSL1 and Sol motor pools in *R4$^{Cre}$::vGlut2$^{flox}$* compared to wild-type mice (Figure 5C).

In summary, genetic perturbation of selective vestibular input channels or muting synaptic output of vestibular neurons result in similar connectivity defects between LVe neurons and flexor motor neurons (Figure 5E). Our observations also reveal that additional factors must play important roles in scaling vestibular input specificity to motor neuron subtypes. Considering the established roles of vestibular and proprioceptive systems in posture and balance, an interesting hypothesis to test is whether these two systems influence each other in establishing their respective connection specificities to motor neurons.

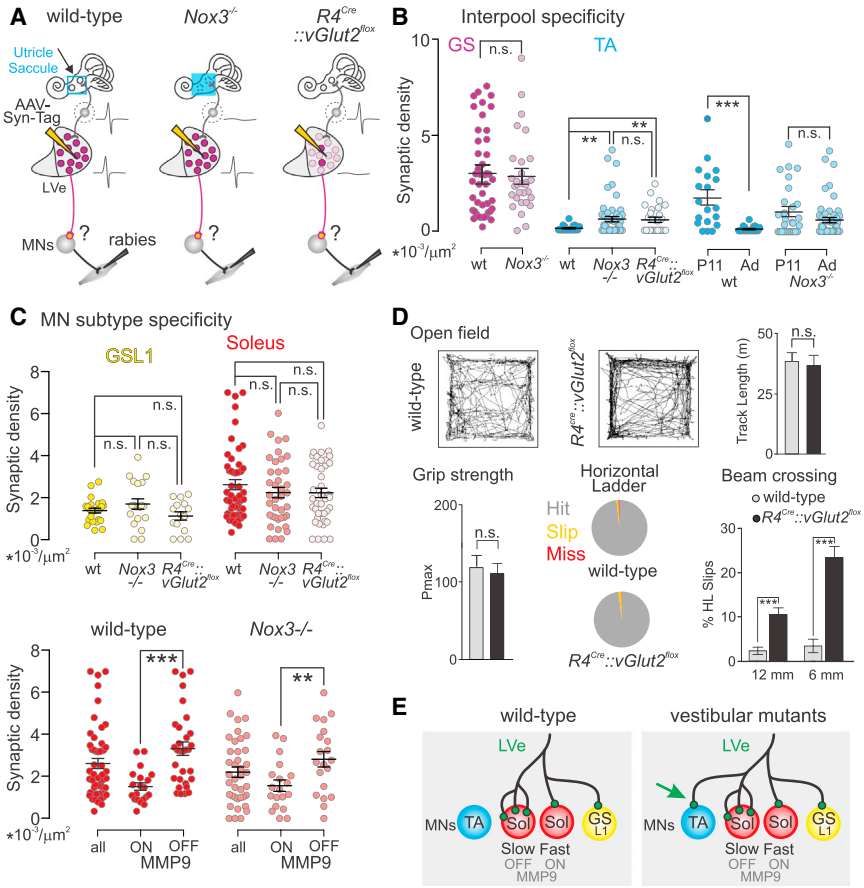


**Figure 5. Perturbation of Vestibular Input Channel Results in Connectivity Defects to Motor Neurons**

(A) Cellular phenotypes and analysis of wild-type, *Nox3*$^{-/-}$, and *R4*$^{Cre}$*::vGlut2*$^{flox}$ mice. *Nox3*$^{-/-}$ mice exhibit defects in otolith-organ derived vestibular sensory input to brainstem vestibular neurons, whereas *R4*$^{Cre}$*::vGlut2*$^{flox}$ mice lack functional output from vestibular neurons to the spinal cord. AAV-Syn-Tag injections are performed to quantify synaptic input density to motor neuron subpopulations.

(B) Synaptic density of LVe input to GS and TA motor neurons at adult (GS, TA) and P11 (TA) stages for wild-type and *Nox3* mutant mice. TA motor neurons were analyzed in adult *R4*$^{Cre}$*::vGlut2*$^{flox}$ mice.

(C) Synaptic density of LVe input to GSL1 and Sol motor neurons in wild-type, *Nox3* mutant, and *R4*$^{Cre}$*::vGlut2*$^{flox}$ mice (top row). Data for Sol motor neurons in wild-type and *Nox3* mutant mice displayed stratified by MMP-9 expression status (bottom row).

(D) Behavioral analysis of wild-type and *R4*$^{Cre}$*::vGlut2*$^{flox}$ mice in open field arena (tracks of individual mice; quantification of track length moved in 10 min), grip strength, horizontal ladder precision (hit, slip, and miss categories displayed in pie chart) and beam crossing on 12 mm- and 6 mm-thick beam.

(E) Summary diagram of synaptic input analyzed between LVe and motor neuron subtypes in wild-type mice and vestibular mutants. Note ectopic synaptic input to TA motor neurons in vestibular mutants.

See also Figure S3.

## Proprioceptive Signaling Influences Vestibular Synaptic Density to Motor Neurons

Given the striking LVe synaptic input variation to different motor neuron subtypes, we first determined the organization of direct synaptic input by proprioceptive afferents to motor neuron subtypes. Of proprioceptors, only muscle spindle afferents connect directly to motor neurons and their synaptic terminals accumulate the vesicular glutamate transporter vGlut1 (Oliveira et al., 2003; Pecho-Vrieseling et al., 2009). Analogous to our analysis of LVe input to motor neuron subtypes (Figure 3), we quantified vGlut1 input density to Chodl$^{ON}$ putative fast motor neurons, Chodl$^{OFF}$ putative slow motor neurons, as well as to identified GSL1 (exclusively FF) and Sol (many slow) motor neurons. We found that vGlut1 input density was higher for GSL1 and Chodl$^{ON}$ motor neurons than for Sol and Chodl$^{OFF}$ putative alpha motor neurons (Figure 6A), a finding opposite to our analysis of input densities derived from the LVe nucleus (Figures 3D and 3E). Moreover, cell body volumes and vGlut1 synaptic input density were positively correlated to each other (Figure 6B), further supporting the notion that fast motor neurons with relatively large cell bodies receive a higher density of vGlut1 inputs than smaller, Chodl$^{OFF}$ alpha motor neurons. Analysis of both LVe and vGlut1 input to the same cohort of motor neurons stratified by Chodl-expression status and cell size confirmed this conclusion (Figures 6C and 6D).

To determine whether the status of proprioceptive input to a motor neuron influences the organization of LVe input to the same motor neuron, we analyzed two mouse mutants with opposite proprioceptive synaptic phenotypes to motor neurons (Figure 7A). *Egr3* mutant mice exhibit early postnatal degeneration of muscle spindles, leading to non-functional muscle spindle afferents (Chen et al., 2002; Tourtellotte and Milbrandt, 1998). In contrast, *Mlc::NT3* mice overexpress NT3 from skeletal muscle fibers, resulting in survival of superfluous proprioceptive afferents with aberrant and more synaptic connections to central synaptic partners (Wang et al., 2007). To assess LVe input to motor neurons in these two mutant mouse strains compared to wild-type mice, we quantified synaptic input to motor neuron cell bodies and dendrites (Figures 7A and 7B).

In *Egr3* mutant mice, we analyzed LVe and vGlut1 input to GSL1 motor neurons, normally exhibiting high-vGlut1 and low-LVe input (Figures 7C–7E). In these mice, vGlut1 contacts to GSL1 motor neurons are present (Figures 7D and 7E) despite their non-functionality (Chen et al., 2002; Tourtellotte and Milbrandt, 1998). However, LVe input to GSL1 motor neurons is significantly increased in *Egr3* mutant mice (Figures 7D and 7E). Conversely, in *Mlc::NT3* mice, we analyzed LVe and vGlut1 input to Sol motor neurons that normally receive relatively low-vGlut1 and high-LVe input (Figures 7F–7H). As expected, Sol motor neurons received significantly more vGlut1

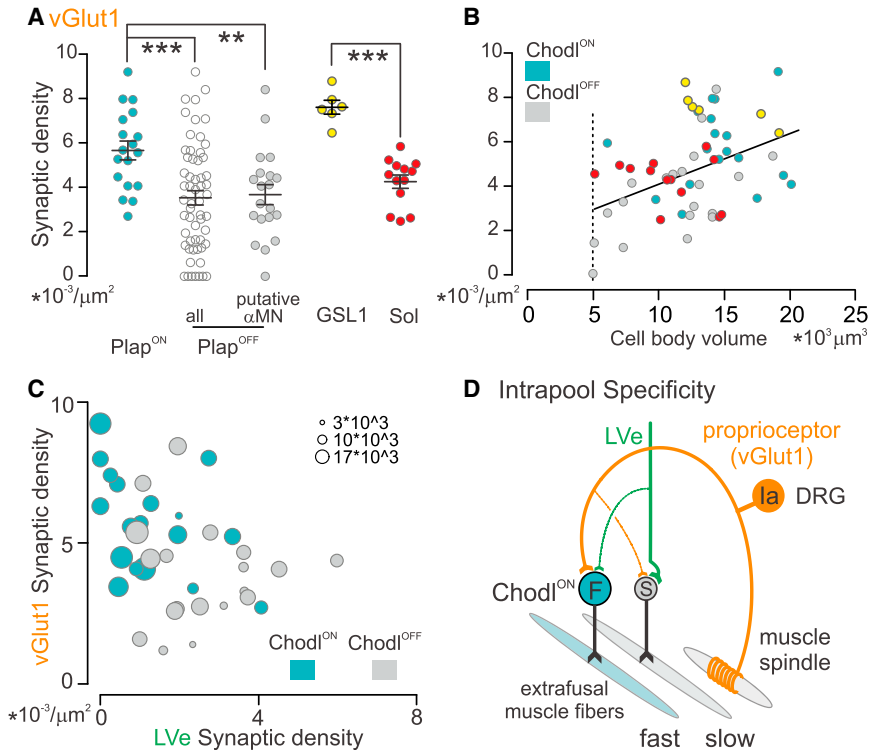


**Figure 6. Vestibular and Proprioceptive Input Anti-correlated by Motor Neuron Subtype**

(A) Density of vGlut1 synaptic input to PLAP$^{ON}$, PLAP$^{OFF}$ (all, or excluding putative gamma motor neurons using a size cut-off criterion of 5,000 µm$^3$), GSL1, and soleus motor neurons.

(B) Synaptic density of vGlut1 input to PLAP$^{ON}$ and putative alpha PLAP$^{OFF}$ motor neurons analyzed in (A) plotted against cell body volumes ($r = 0.448$, $p = 0.0054$). GSL1 and Sol motor neurons are also displayed in this plot but not included in the correlation analysis.

(C) Plot of vGlut1 versus LVe synaptic input density to PLAP$^{ON}$ and putative alpha PLAP$^{OFF}$ motor neurons in relation to cell body volume illustrated by diameter of plotted circles.

(D) Intrapool stratification of LVe and Ia proprioceptive vGlut1 input to fast (F, ChodI$^{ON}$) and slow (S, ChodI$^{OFF}$) alpha motor neurons, revealing anti-correlated synaptic input densities.

input in *MLC::NT3* than wild-type mice, but LVe input density was strongly reduced (Figures 7G and 7H). Despite these differences in LVe connectivity to motor neuron subtypes however, overall LVe synaptic patterns in the spinal cord were not perturbed across genotypes and injection conditions (Figure S4).

To determine whether the lack of direct functional proprioceptive input to motor neurons in *Egr3* mutant mice also influences LVe input to flexor motor neurons, we next compared input to TA motor neurons between wild-type and *Egr3* mutant mice. We found that there was no significant difference between genotypes (Figures S5A–S5D). These results demonstrate that altered proprioceptive signaling to flexor motor neurons cannot overrule the scarcity of LVe input to these neurons. Thus, the assembly of LVe inputs at the motor pool and motor neuron subtype level employs distinct developmental mechanisms.

Lastly, to test whether the synaptic scaling of these two complementary sensory systems operates bidirectionally, i.e., whether altered LVe input scales vGlut1 input to motor neurons, we analyzed vGlut1 input to Sol motor neurons in *Nox3* mutant mice. We detected a striking increase in vGlut1 terminals to Sol motor neurons in these mutants compared to wild-type mice (Figures S6A and S6B). This finding suggests that LVe signaling influences the scaling of proprioceptive inputs to motor neurons.

## DISCUSSION

The control of posture and balance is essential for motor performance. The vestibular system plays an important role in this process through its ability to stabilize and adjust body position during movement (Angelaki and Cullen, 2008; Grillner et al., 1970; Wilson and Yoshida, 1968). Using genetic perturbation experiments, we demonstrate that signaling interactions between the proprioceptive and vestibular system play a key role in shaping connection specificity between vestibular neurons in the brainstem and spinal motor neurons. We discuss how these findings advance our understanding of vestibular system function, especially in the context of connectivity refinement and functional interaction with proprioceptive circuitry to ensure smooth motor behavior.

### Motor Neuron Subtype Identity Aligns with Synaptic Input Specificity

Work on the cat lumbar spinal cord demonstrates that select lumbar extensor motor pools are favored direct synaptic targets for LVe input compared to flexor counterparts (Grillner et al., 1970), a profile we find to be conserved in mice. A key insight of our work is that the observed extensor-flexor interpool specificity pattern is supplemented by a preference of LVe input to target slow over fast motor neuron subtypes within each extensor pool analyzed, and notably, this bias is even detectable at the level of a general lumbar LMC motor neuron analysis.

What may be the functional reasons behind the identified vestibulo-motor connectivity profile to preferentially target slow over fast motor neurons within extensor pools? Vestibular input enhances the activation of motor neurons innervating extensor muscles exhibiting antigravitational function and can produce large motoneuronal depolarizations through temporal summation (Grillner et al., 1970). This is physiologically relevant since vestibular neurons fire at high frequencies (Angelaki and Cullen, 2008), also detected in awake behaving mice (Beraneck and Cullen, 2007), demonstrating that the vestibular system has

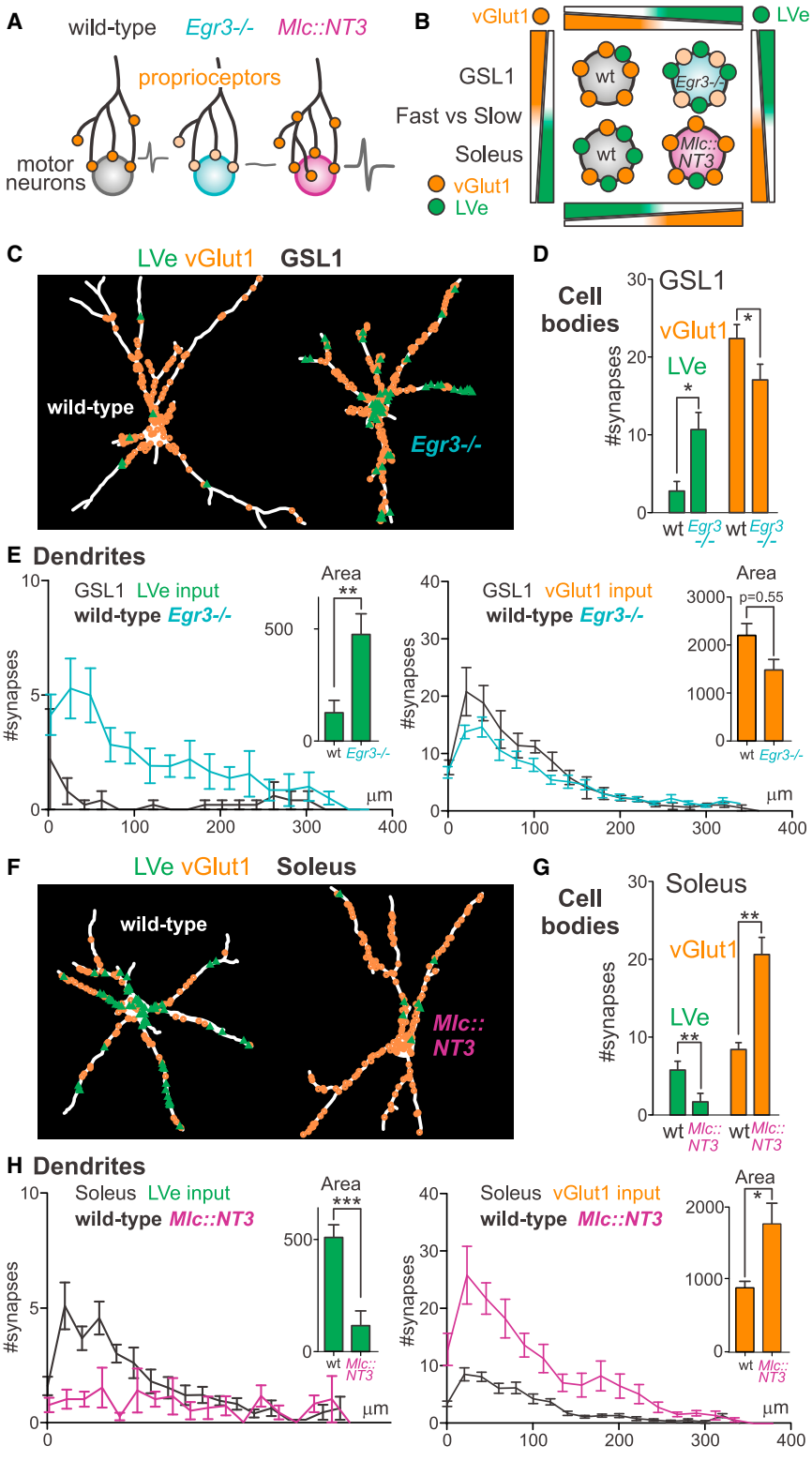


**Figure 7. Muscle Spindle Signaling Influences Input to Motor Neuron Subtypes**

(A) Synaptic input status of proprioceptors to alpha motor neurons in wild-type, *Egr3*$^{-/-}$ and *MLC::NT3* mice. *Egr3*$^{-/-}$ proprioceptive terminals are physically present but non-functional, whereas they show over-proliferation and aberrant connections in *MLC::NT3* mice.

(B) Summary diagram illustrating main findings. LVe inputs to motor neuron subtypes of extensor pools are affected by genetic manipulation of proprioceptor input function.

(C–H) Neurolucida reconstruction (C and F) and quantification (D, E, G, and H) of LVe and vGlut1 synaptic input to GSL1 and soleus motor neurons in wild-type, compared to *Egr3*$^{-/-}$ (for GSL1) and *MLC::NT3* (for soleus) mice both at the cell body (D and G) and dendrite (D and H) level. In (E) and (H) area under curves are quantified and shown in bar graphs.

See also Figures S4, S5, and S6.

subtypes selectively recruited during endurance and postural tasks and with the ability to support contractions without fatigue (Burke, 1967; Kanning et al., 2010). In contrast, fast motor neurons receive sparse direct vestibular input, in line with these motor neurons being recruited during fast and powerful muscle contractions but to fatigue quickly (Burke, 1967; Kanning et al., 2010).

Our work is focused on synaptic input specificity directly to motor neurons, but vestibular signaling also acts through indirect pathways via spinal interneurons, and these pathways also employ specific connectivity rules following motor pool-specific patterns (Grillner et al., 1970). Even though flexor motor pools do not receive direct excitatory LVe inputs, disynaptic pathways can specifically inhibit them and thereby further enhance the differential functional impact that LVe signaling exhibits on extensor and flexor motor pools. Electrophysiological studies on the organization of peripheral and rubrospinal inputs to motor neurons demonstrate that indirect inputs can also exhibit fiber-type-specific functional connectivity profiles (Burke et al., 1970). Whether indirect inputs to motor neurons in the vestibular system also follow the intrapool motor unit twitch-type organizational principle as direct ones do will be an interesting question to pursue.

the capability to contribute to motoneuronal recruitment. Our work shows that the vestibular system contributes to this process by preferential targeting of slow extensor motor neuron

### Multisensory Integration in the Motor Output System

The functionality of the motor system depends heavily on continuous integration of sensory information of different modalities. Multisensory inputs influence many neuronal elements along motor output pathways, a general organizational principle that is evolutionarily conserved even to circuits regulating *Drosophila* larvae behavior (Ohyama et al., 2015). Focusing on the last synapse of motor output pathways affecting movement, we found that vestibular and proprioceptive inputs converge on slow and fast motor neuron subtypes with an inverse anatomical synaptic scaling profile. While we favor the view that functional complementarity plays a role in synaptic scaling, whether similar scaling processes can also occur between functionally non-complementary inputs remains to be determined.

Our findings raise the question of how and where proprioceptive and vestibular systems interact functionally. Most relevant for our study, the vestibular system can enhance proprioceptive inputs in a synergistic manner (Grillner et al., 1970). Moreover, vestibular input to motor neurons inherently carries multisensory information. Vestibular neurons are secondary neurons in the chain of sensory input processing, receiving primary vestibular sensory input as well as indirect feedback from the proprioceptive and visual system (Angelaki and Cullen, 2008). In particular, somatosensory feedback circuits activated by passive hindlimb movement regulate vestibular neuron activity (Arshian et al., 2014). Thus direct vestibular input to motor neurons combines multiple sensory streams of different degrees of integration and we found that these inputs are organized into precise patterns and are complementary to direct proprioceptive inputs.

### Developmental Mechanisms Guiding the Assembly of Inputs to Motor Neurons

The precise developmental assembly of synaptic inputs to motor neurons is a prerequisite for the functionality of the mature motor system. Despite its importance however, mechanistic insight exists for only a limited number of functionally defined neuronal subpopulations with synaptic access to motor neurons. The wiring specificity between proprioceptors and motor neuron pools within the same reflex arc is established early and through mechanisms independent of neuronal activity (Frank, 1990; Mears and Frank, 1997). Combinatorial action of neuronal and retrograde molecular factors as well as positional cues play important roles in instructing sensory-motor connectivity (Arber, 2012; Wenner and Frank, 1995). Yet sensory connectivity to synergistic motor pools refines at postnatal stages, a process influenced by proprioceptor neuron activity (Mendelsohn et al., 2015).

Here, we have assessed time course and mechanisms of vestibular input assembly and refinement to motor neurons. We found that while significant input differences between extensor (GS) and flexor (TA) motor neurons are already established at early postnatal stages, a likely activity-dependent postnatal synaptic refinement process abolishes vestibular input to TA motor neurons. We revealed that this process is driven at least in part by vestibular signaling itself. The time window during which refinement occurs (P11–P17) matches the emergence of posture and weight bearing in rodents (Geisler et al., 1993), raising the possibility that maturation of synaptic input may be linked to the emergence of postural behavioral abilities.

The second level of synaptic input scaling to motor neuron subtypes is shaped by bidirectional sensory signaling. Genetic manipulations affecting either the functionality of muscle spindle feedback or vestibular signaling resulted in adjustments of the other channel counterbalancing the genetically imposed changes. How could such input adjustment to motor neurons be regulated? We found that in mice, proprioceptive connections exhibit higher proximal synaptic input with gradually decreasing input on distal dendrites, in agreement with recent input reconstructions to rat motor neurons (Rotterman et al., 2014). Interestingly, compensatory LVe input distribution to GSL1 FF motor neurons in *Egr3* mutant mice scales accordingly. Since these muscle spindle afferent synapses are present but non-functional (Chen et al., 2002), it is likely that the observed adjustment of synaptic input to motor neurons is not merely a competition for synaptic space. A plausible mechanism instead might be that synaptic input to motor neurons is regulated locally through retrograde and homeostatic mechanisms involving postsynaptic feedback from motor neurons. In this context, it is interesting to consider that individual group Ia afferents connect to almost all motor neurons supplying the same muscle (Mendell and Henneman, 1968). Ia input density scaling therefore likely occurs at the level of individual motor neurons according to subtype identity. Moreover, proprioceptor-driven vestibular synaptic scaling only operates on motor neuron pools to which LVe input has direct functional impact, as we observed no input scaling to TA motor neurons that receive proprioceptive but are devoid of LVe input. Thus, the two studied sensory channels differentially influence the refinement and scaling process of inputs to motor neurons, further supporting the idea that multiple independent layers regulate input specificity to motor neuron subtypes.

Bidirectional synaptic compensation may also explain at least part of the relatively minor locomotor phenotypes observed in *Egr3* mutants (Takeoka et al., 2014) and $R4^{Cre}$::$vGlut2^{flox}$ mice analyzed here, both of which exhibit signaling defects in the respective sensory system starting during development. Interestingly, cross-modal sensory regulation during development also appears to operate in humans. Patients with infant-onset vestibular system dysfunction show limited behavioral abnormalities likely due to somatosensory compensatory mechanism, whereas compensation following adult injury to the vestibular system is restricted (Horak et al., 1994). These observations suggest that there might be a developmentally defined critical period for cross-modal sensory regulation to adjust circuitry to motor neurons needed for posture and balance. Together, our work uncovers how sensory inputs of functionally complementary modality converge and influence each other at the final output step controlling movement, providing an important contribution to understanding specificity and function of the motor system.

## EXPERIMENTAL PROCEDURES

### Mouse Genetics

$Tau^{lox\text{-}STOP\text{-}lox\text{-}Flp\text{-}INLA}$ (Pivetta et al., 2014), $Chodl^{PLAP}$ (Sakurai et al., 2013), *NADPH oxidase 3* (*Nox3*) mutant (Paffenholz et al., 2004), $vGlut2^{flox}$ (Jax Mice Strain #007583), *Egr3* mutant (Tourtellotte and Milbrandt, 1998), $R4^{Cre}$ (Di Bonito et al., 2013), and *Mlc::NT3* (Wang et al., 2007) mouse strains were maintained on a mixed genetic background (129/C57Bl6). Housing, surgery,

behavioral experiments and euthanasia were performed in compliance with the Swiss Veterinary Law guidelines.

### Virus Production and Injections

Rabies viruses (Rabies-mCherry and Rabies-GFP: Rabies-FP) used were amplified and purified from local viral stocks following established protocols (Stepien et al., 2010; Wickersham et al., 2007). All AAVs used in this study were described previously (Esposito et al., 2014; Pivetta et al., 2014; Takeoka et al., 2014) and of genomic titers >1 × 10e13. Additional information on anterograde and retrograde viral tracing, immunohistochemistry, imaging and anatomical quantification are found in the Supplemental Experimental Procedures.

### Behavioral Analysis

Open field, grip strength test, horizontal ladder locomotion, and beam tests were performed as previously described (Esposito et al., 2014; Takeoka et al., 2014; Carter et al., 2001). Additional information on detailed behavioral analyses is found in the Supplemental Experimental Procedures.

### Statistics

All statistical analysis, plots, and linear regression lines were made using GraphPad PRISM (v6.0). Column bar graphs and dot plots represent the average value ± SEM. The means of different data distributions were compared using an unpaired Student's t test (Figures 1D, 1F, 1H, 2A, 2D, 3D, 3F, 4B, 4D, 5B–5D, 6A, 7D, 7G, S3, S4, S5B, and S6A). Correlation analysis was used for Figures 3E and 6B. A one-way ANOVA for independent measurements was used for comparing multiple TA datasets in Figure 4B. The area under the frequency-distribution curves in Figures 7I, 7H, S5, and S6B was used as a measure of synaptic input on dendrites. The correlogram plot shown in Figure 6C was obtained in R using the library ggplot. Significance level is defined as follows for all analyses performed: $^{*}p < 0.05$; $^{**}p < 0.01$; $^{***}p < 0.001$.

## SUPPLEMENTAL INFORMATION

Supplemental Information includes Supplemental Experimental Procedures and six figures and can be found with this article online at http://dx.doi.org/10.1016/j.cell.2015.09.023.

## ACKNOWLEDGMENTS

We are grateful to M. Mielich for expert technical help, M. Tripodi for help and guidance during initial stages of the project, F. Roselli for insights into motor neuron subtypes and muscle subcompartments, M. Studer for sharing *R4::Cre* mice with us, S. Bourke, C. Genoud, and L. Gelman from the FMI imaging facility, N. Ehrenfurchter from the Biozentrum Imaging facility and M. Stadler from the FMI Bioinformatics Platform for help and advice with image acquisition and analysis, and to P. Caroni and B. Roska for discussions and comments on the manuscript. E.B. was supported by a fellowship of the Werner Siemens Foundation, A.T. by an International Foundation for Research in Paraplegia (IRP) fellowship. All authors were supported by an ERC Advanced Grant, the Swiss National Science Foundation, the Kanton Basel-Stadt, and the Novartis Research Foundation.

Received: July 8, 2015
Revised: August 22, 2015
Accepted: September 1, 2015
Published: October 8, 2015

## REFERENCES

Abraira, V.E., and Ginty, D.D. (2013). The sensory neurons of touch. Neuron *79*, 618–639.

Angelaki, D.E., and Cullen, K.E. (2008). Vestibular system: the many facets of a multimodal sense. Annu. Rev. Neurosci. *31*, 125–150.

Arber, S. (2012). Motor circuits in action: specification, connectivity, and function. Neuron *74*, 975–989.

Arshian, M.S., Hobson, C.E., Catanzaro, M.F., Miller, D.J., Puterbaugh, S.R., Cotter, L.A., Yates, B.J., and McCall, A.A. (2014). Vestibular nucleus neurons respond to hindlimb movement in the decerebrate cat. J. Neurophysiol. *111*, 2423–2432.

Beraneck, M., and Cullen, K.E. (2007). Activity of vestibular nuclei neurons during vestibular and optokinetic stimulation in the alert mouse. J. Neurophysiol. *98*, 1549–1565.

Brodal, A., and Pompeiano, O. (1957). The vestibular nuclei in cat. J. Anat. *91*, 438–454.

Brown, A.G. (1981). Organization of the Spinal Cord (Springer Verlag).

Burke, R.E. (1967). Motor unit types of cat triceps surae muscle. J. Physiol. *193*, 141–160.

Burke, R.E., Jankowska, E., and ten Bruggencate, G. (1970). A comparison of peripheral and rubrospinal synaptic input to slow and fast twitch motor units of triceps surae. J. Physiol. *207*, 709–732.

Burke, R.E., Dum, R.P., Fleshman, J.W., Glenn, L.L., Lev-Tov, A., O'Donovan, M.J., and Pinter, M.J. (1982). A HRP study of the relation between cell size and motor unit type in cat ankle extensor motoneurons. J. Comp. Neurol. *209*, 17–28.

Carter, R.J., Morton, J., and Dunnett, S.B. (2001). Motor coordination and balance in rodents. Curr. Protoc. Neurosci. *Chapter 8*, Unit 8.12.

Chen, H.H., Tourtellotte, W.G., and Frank, E. (2002). Muscle spindle-derived neurotrophin 3 regulates synaptic connectivity between muscle sensory and motor neurons. J. Neurosci. *22*, 3512–3519.

Di Bonito, M., Narita, Y., Avallone, B., Sequino, L., Mancuso, M., Andolfi, G., Franzè, A.M., Puelles, L., Rijli, F.M., and Studer, M. (2013). Assembly of the auditory circuitry by a Hox genetic network in the mouse brainstem. PLoS Genet. *9*, e1003249.

Du Beau, A., Shakya Shrestha, S., Bannatyne, B.A., Jalicy, S.M., Linnen, S., and Maxwell, D.J. (2012). Neurotransmitter phenotypes of descending systems in the rat lumbar spinal cord. Neuroscience *227*, 67–79.

Eccles, J.C., Eccles, R.M., and Lundberg, A. (1957). The convergence of monosynaptic excitatory afferents on to many different species of alpha motoneurones. J. Physiol. *137*, 22–50.

Enjin, A., Rabe, N., Nakanishi, S.T., Vallstedt, A., Gezelius, H., Memic, F., Lind, M., Hjalt, T., Tourtellotte, W.G., Bruder, C., et al. (2010). Identification of novel spinal cholinergic genetic subtypes disclose Chodl and Pitx2 as markers for fast motor neurons and partition cells. J. Comp. Neurol. *518*, 2284–2304.

Esposito, M.S., Capelli, P., and Arber, S. (2014). Brainstem nucleus MdV mediates skilled forelimb motor tasks. Nature *508*, 351–356.

Frank, E. (1990). The formation of specific synaptic connections between muscle sensory and motor neurons in the absence of coordinated patterns of muscle activity. J. Neurosci. *10*, 2250–2260.

Geisler, H.C., and Gramsbergen, A. (1998). Motor development after vestibular deprivation in rats. Neurosci. Biobehav. Rev. *22*, 565–569.

Geisler, H.C., Westerga, J., and Gramsbergen, A. (1993). Development of posture in the rat. Acta Neurobiol. Exp. (Warsz.) *53*, 517–523.

Grillner, S., and Dubuc, R. (1988). Control of locomotion in vertebrates: spinal and supraspinal mechanisms. Adv. Neurol. *47*, 425–453.

Grillner, S., Hongo, T., and Lund, S. (1970). The vestibulospinal tract. Effects on alpha-motoneurones in the lumbosacral spinal cord in the cat. Exp. Brain Res. *10*, 94–120.

Horak, F.B., Shupert, C.L., Dietz, V., and Horstmann, G. (1994). Vestibular and somatosensory contributions to responses to head and body displacements in stance. Exp. Brain Res. *100*, 93–106.

Kanning, K.C., Kaplan, A., and Henderson, C.E. (2010). Motor neuron diversity in development and disease. Annu. Rev. Neurosci. *33*, 409–440.

Kaplan, A., Spiller, K.J., Towne, C., Kanning, K.C., Choe, G.T., Geber, A., Akay, T., Aebischer, P., and Henderson, C.E. (2014). Neuronal matrix metalloproteinase-9 is a determinant of selective neurodegeneration. Neuron *81*, 333–348.

Leroy, F., Lamotte d'Incamps, B., Imhoff-Manuel, R.D., and Zytnicki, D. (2014). Early intrinsic hyperexcitability does not contribute to motoneuron degeneration in amyotrophic lateral sclerosis. eLife *3*, 3.

Liang, H., Bácskai, T., Watson, C., and Paxinos, G. (2014). Projections from the lateral vestibular nucleus to the spinal cord in the mouse. Brain Struct. Funct. *219*, 805–815.

Liang, H., Bácskai, T., and Paxinos, G. (2015). Termination of vestibulospinal fibers arising from the spinal vestibular nucleus in the mouse spinal cord. Neuroscience *294*, 206–214.

Lund, S., and Pompeiano, O. (1968). Monosynaptic excitation of alpha motoneurones from supraspinal structures in the cat. Acta Physiol. Scand. *73*, 1–21.

Lundberg, A. (1975). Control of spinal mechanisms from the brain. In The Basic Neurosciences (Raven Press).

Matthews, P.B. (1981). Evolving views on the internal operation and functional role of the muscle spindle. J. Physiol. *320*, 1–30.

Mears, S.C., and Frank, E. (1997). Formation of specific monosynaptic connections between muscle spindle afferents and motoneurons in the mouse. J. Neurosci. *17*, 3128–3135.

Mendell, L.M., and Henneman, E. (1968). Terminals of single Ia fibers: distribution within a pool of 300 homonymous motor neurons. Science *160*, 96–98.

Mendelsohn, A.I., Simon, C.M., Abbott, L.F., Mentis, G.Z., and Jessell, T.M. (2015). Activity regulates the incidence of heteronymous sensory-motor connections. Neuron *87*, 111–123.

Moorman, S.J., Cordova, R., and Davies, S.A. (2002). A critical period for functional vestibular development in zebrafish. Dev. Dyn. *223*, 285–291.

Ohyama, T., Schneider-Mizell, C.M., Fetter, R.D., Aleman, J.V., Franconville, R., Rivera-Alba, M., Mensh, B.D., Branson, K.M., Simpson, J.H., Truman, J.W., et al. (2015). A multilevel multimodal circuit enhances action selection in Drosophila. Nature *520*, 633–639.

Oliveira, A.L., Hydling, F., Olsson, E., Shi, T., Edwards, R.H., Fujiyama, F., Kaneko, T., Hökfelt, T., Cullheim, S., and Meister, B. (2003). Cellular localization of three vesicular glutamate transporter mRNAs and proteins in rat spinal cord and dorsal root ganglia. Synapse *50*, 117–129.

Paffenholz, R., Bergstrom, R.A., Pasutto, F., Wabnitz, P., Munroe, R.J., Jagla, W., Heinzmann, U., Marquardt, A., Bareiss, A., Laufs, J., et al. (2004). Vestibular defects in head-tilt mice result from mutations in Nox3, encoding an NADPH oxidase. Genes Dev. *18*, 486–491.

Pecho-Vrieseling, E., Sigrist, M., Yoshida, Y., Jessell, T.M., and Arber, S. (2009). Specificity of sensory-motor connections encoded by Sema3e-Plxnd1 recognition. Nature *459*, 842–846.

Pivetta, C., Esposito, M.S., Sigrist, M., and Arber, S. (2014). Motor-circuit communication matrix from spinal cord to brainstem neurons revealed by developmental origin. Cell *156*, 537–548.

Pun, S., Santos, A.F., Saxena, S., Xu, L., and Caroni, P. (2006). Selective vulnerability and pruning of phasic motoneuron axons in motoneuron disease alleviated by CNTF. Nat. Neurosci. *9*, 408–419.

Rotterman, T.M., Nardelli, P., Cope, T.C., and Alvarez, F.J. (2014). Normal distribution of VGLUT1 synapses on spinal motoneuron dendrites and their reorganization after nerve injury. J. Neurosci. *34*, 3475–3492.

Sakurai, K., Akiyama, M., Cai, B., Scott, A., Han, B.X., Takatoh, J., Sigrist, M., Arber, S., and Wang, F. (2013). The organization of submodality-specific touch afferent inputs in the vibrissa column. Cell Rep. *5*, 87–98.

Shinoda, Y., Ohgaki, T., Futami, T., and Sugiuchi, Y. (1988). Vestibular projections to the spinal cord: the morphology of single vestibulospinal axons. Prog. Brain Res. *76*, 17–27.

Stepien, A.E., Tripodi, M., and Arber, S. (2010). Monosynaptic rabies virus reveals premotor network organization and synaptic specificity of cholinergic partition cells. Neuron *68*, 456–472.

Takeoka, A., Vollenweider, I., Courtine, G., and Arber, S. (2014). Muscle spindle feedback directs locomotor recovery and circuit reorganization after spinal cord injury. Cell *159*, 1626–1639.

Tourtellotte, W.G., and Milbrandt, J. (1998). Sensory ataxia and muscle spindle agenesis in mice lacking the transcription factor Egr3. Nat. Genet. *20*, 87–91.

Uchino, Y., and Kushiro, K. (2011). Differences between otolith- and semicircular canal-activated neural circuitry in the vestibular system. Neurosci. Res. *71*, 315–327.

Van Cleave, S., and Shall, M.S. (2006). A critical period for the impact of vestibular sensation on ferret motor development. J. Vestib. Res. *16*, 179–186.

Walton, K.D., Harding, S., Anschel, D., Harris, Y.T., and Llinás, R. (2005). The effects of microgravity on the development of surface righting in rats. J. Physiol. *565*, 593–608.

Wang, Z., Li, L.Y., Taylor, M.D., Wright, D.E., and Frank, E. (2007). Prenatal exposure to elevated NT3 disrupts synaptic selectivity in the spinal cord. J. Neurosci. *27*, 3686–3694.

Wenner, P., and Frank, E. (1995). Peripheral target specification of synaptic connectivity of muscle spindle sensory neurons with spinal motoneurons. J. Neurosci. *15*, 8191–8198.

Wickersham, I.R., Lyon, D.C., Barnard, R.J., Mori, T., Finke, S., Conzelmann, K.K., Young, J.A., and Callaway, E.M. (2007). Monosynaptic restriction of transsynaptic tracing from single, genetically targeted neurons. Neuron *53*, 639–647.

Wilson, V.J., and Yoshida, M. (1968). Vestibulospinal and reticulospinal effects on hindlimb, forelimb, and neck alpha motoneurons of the cat. Proc. Natl. Acad. Sci. USA *60*, 836–840.

Windhorst, U. (2007). Muscle proprioceptive feedback and spinal networks. Brain Res. Bull. *73*, 155–202.